

## SEISMIC SIGNAL PROCESSING

The seismic method, considered as an instrument for remote detection, has much in common with other disciplines that use noninvasive techniques to find the structure of an inaccessible body. For example, the methods described here are especially applicable to ultrasonic medical imaging and non-destructive evaluation. An important use of seismic signal processing is to look beneath the surface of the earth in the search for new deposits of oil and natural gas. The subsurface geologic structures of interest can be as deep as 8 km. The exploration geophysicist illuminates the subsurface by means of a energy source that generates seismic waves. The subsurface rock layers transmit and reflect the seismic waves. A seismic survey consists in collecting data over a selected geographic area, called the *prospect*.

Essential features of seismic data acquisition are: At a fixed point on the surface of the earth, a source of energy, such as arrays of dynamite charges, or air guns, or chirp-signal (vibroseis) generators, is activated. An activated source is called a *shot*. Seismic waves from the shot propagate downward from the source point deep into the earth. The waves are reflected from geologic interfaces. The reflected waves propagate upward from these interfaces. A primary reflection is a reflection that travels directly down to the interface, and then directly back up to the surface. A multiple reflection is a reflection that bounces back and forth among various inter-

faces as it proceeds on its trip. The reflected waves, both primaries and multiples, are detected on the surface by receivers. The receiver points are located at various horizontal distances from the source point. The digitized signal recorded at each receiver point for a given source point is called a *trace*. After one shot is completed, the source point and the corresponding receiver points are moved so that another shot can take place. This procedure is repeated until the entire prospect is covered.

It is not economically feasible to make a nearly continuous survey. Instead, within the confines of a given exploration budget, a fixed number of source and receiver points must be used. The points are chosen so as to obtain the best possible representation of the prospect. Such a procedure represents sampling in the space domain. The traces as recorded by the receivers constitute the raw data, which are then fed into computers for processing. The purpose of digital seismic processing is to transform the raw data into computer-generated images of the subsurface geological structures. The high dynamic range of the receivers available today makes possible the use of precise signal processing methods that give excellent image quality. The images, in the form of maps and cross sections, are then interpreted by geologists and geophysicists in order to choose the most favorable drilling sites for new oil wells, either wildcats or field-extension wells.

Geophysical theory deals with both forward problems and inverse problems. In a forward problem the mathematical model of the energy source and the transmission medium are given. It is desired to find what the resulting received data would be. In other words, the forward problem goes from the source through the medium to the data. The forward problem corresponds to what occurs in nature. In geophysical exploration, on the other hand, one is faced with an inverse problem. The received data are the traces recorded at the surface of the earth. From these data it is desired to find the subsurface geologic structure. Thus the inverse problem starts with the received data and extrapolates backward in time through the geologic medium toward the source. Inverse problems fall into the categories of inverse source problems and inverse medium problems. Generally speaking, the seismic inverse problem may be regarded as an inverse medium problem. The desired information is the structure of the medium through which the seismic waves travel.

The seismic reflection method was perfected for petroleum exploration in the 1920s. During the period from 1930 to 1950, the seismic reflection method revolutionized oil exploration. The raw data were recorded (in real time) as traces on photographic paper. In this precomputer era, the raw data were visually inspected by geophysicists in order to mark primary reflected events that had continuity from trace to trace. The subsurface maps were determined from plotting the horizons that would give rise to these primary reflections. By 1950, sophisticated analog filters were being applied to the received signals before they were recorded as traces. Despite these advances, many—in fact, most—of the great potential oil-producing regions of the world had to be abandoned as active areas of exploration. Seismic records from such areas were classified as NG (no good) because the raw data did not reveal primary reflections that could be picked visually from trace to trace. The general belief was that valid primary reflection events were indeed present on NG records, but were hidden from view by various types of noise, including multiple

reflections. The outstanding problem was to find a way to uncover the hidden primary reflection events on NG records. Despite great efforts in instrumentation, encouraging results from the use of various types of analog filters were not forthcoming. Urged by Prof. Norbert Wiener, the petroleum industry supported research on digital signal processing in the MIT Mathematics Department starting in the fall of 1950. Although Wiener was primarily a pure mathematician, his inner heart was directed toward applications (1,2). The result of this research effort was the development of the method of *deconvolution* (3). It was applied to NG exploration records and was successful in bringing out reflections that otherwise could not be seen.

Deconvolution was a digital method that required a digital computer for implementation. Initially the Whirlwind computer at MIT and the Ferranti computer at the University of Toronto were used, but such vacuum-tube computers did not have the power to process the great numbers of seismic records taken in an active exploration program. The introduction of transistorized computers in the late 1950s dramatically changed the situation, and the oil exploration industry started to use deconvolution commercially. Difficult areas on land yielded up their secrets. Because deconvolution was able to remove water-layer reverberations, the offshore regions of the world were at last opened up for oil exploration. The impetus resulting from great oil discoveries in these previously unattainable areas produced a digital revolution in geophysics in the early 1960s. From that time on, digital signal processing has been the rule in every oil exploration program.

## WAVELETS

Much of geophysical signal processing is concerned with the manipulation of wavelets (4). In geophysics, a wavelet is a signal that has finite energy. In other words, a wavelet is a transient phenomenon, with the bulk of its energy confined to a finite interval on the time scale. An important subgroup of wavelets is made up of those wavelets that have a finite number of coefficients, that is, wavelets that have finite length. A finite-length wavelet  $b$  of length  $m + n + 1$  is given by

$$b = \{b_{-m}, \dots, b_{-2}, b_{-1}, b_0, b_1, b_2, \dots, b_n\}$$

where the coefficient  $b_0$  occurs at time index 0. The causal part is made up of those coefficients occurring from time index 0 onward, and the noncausal part is made up of those coefficients occurring before time index 0. The time reverse is obtained by reflecting the wavelet about the zero time index; that is, the time reverse is

$$b^R = \{b_n, \dots, b_2, b_1, b_0, b_{-1}, b_{-2}, \dots, b_{-m}\}$$

where the coefficient  $b_0$  still occurs at time index 0. The coefficients with positive indices are now noncausal, and the coefficients with negative indices are now causal. A finite-length causal wavelet could be

$$\{b_0, b_1, b_2, \dots, b_n\}$$

where the coefficient  $b_0$  occurs at time index 0. Because all coefficients of a causal wavelet before time index 0 are zero, a causal wavelet is said to be one-sided. Its reverse is

$$b^R = \{b_n, \dots, b_2, b_1, b_0\}$$

where the coefficient  $b_0$  occurs at time index 0. Such a wavelet is anticausal. An anticausal wavelet also has the one-sided property, but in the opposite time direction. All coefficients of an anticausal wavelet occurring after time index 0 are zero.

The *delayed reverse* is obtained by shifting the coefficients of the reverse wavelet far enough to the right to make the result causal. It is given by

$$b^{DR} = \{b_n, \dots, b_2, b_1, b_0\}$$

where now the coefficient  $b_n$  occurs at time index 0.

A centered asterisk denotes convolution: the convolution of two wavelets, say  $a$  and  $b$ , is denoted by  $a * b$ . The *autocorrelation* of a wavelet is given by the convolution of the wavelet with its reverse; that is, the autocorrelation of  $a$  is  $a * a^R$ . The *cross-correlation* of the wavelet  $a$  with the wavelet  $b$  is given by  $a * b^R$ . The autocorrelation and cross-correlation as defined here are unnormalized.

In certain key places, the conventions used in signal processing by geophysicists and by electrical engineers differ. It is good to point out the differences at the outset in order to make the geophysical literature more accessible. Geophysicists and electrical engineers have different conventions with respect to the  $z$  transform. Let  $h_0, h_1, h_2, \dots$  be the impulse response of a causal time-invariant linear filter. The engineering  $z$  transform is

$$H_e(z) = h_0 + h_1z^{-1} + h_2z^{-2} + \dots$$

whereas the geophysics  $Z$  transform is

$$H(Z) = h_0 + h_1Z + h_2Z^2 + \dots$$

The two are related by  $Z = z^{-1}$ . Whereas the engineering  $z$  represents a unit-advance operator, the geophysics  $Z$  represents a unit-delay operator.

The  $Z$  transform of the impulse response of a filter is called its *transfer function*. A stable causal time-invariant linear filter is said to be (strictly) minimum-delay (or minimum-phase) if the zeros (or roots) of its transfer function lie outside the unit circle (5). An alternative characterization is that a filter is minimum-phase when it is stable with a stable inverse. At any frequency, a minimum-phase filter has a smaller phase-shift than that of any other filter with the same amplitude spectrum. Also the impulse response of minimum-phase filter has a faster energy buildup as compared to that of any other filter with the same amplitude spectrum. The inverse of a minimum-delay filter  $H^{-1}(Z) = 1/H(Z)$  is also minimum-delay. The transfer function of a causal finite impulse response (FIR) filter is the polynomial

$$H(Z) = h_0 + h_1Z + \dots + h_mZ^m$$

An important type of stable causal infinite impulse response (IIR) filter is the recursive filter with transfer function given by the rational function  $H(Z) = B(Z)/A(Z)$  with the provision that the denominator polynomial  $A(Z)$  is minimum-delay. This provision ensures that the recursive filter is stable. The locations of the zeros of the numerator polynomial  $B(Z)$  do not need to be specified in order for the recursive filter to be stable. However, if it is further specified that the numerator polynomial  $B(Z)$  is minimum-delay, then the recursive fil-

ter is minimum-delay. Reference is made to the excellent treatment of linear time-invariant discrete-time systems given by Bose (6).

The delayed reverse of a finite-length minimum-delay wavelet is said to be maximum-delay. An example of a minimum-delay wavelet is  $\{0, 7, 3\}$ , where the coefficient 7 occurs at time index 0 and the coefficient 3 occurs at time index 1. Its reverse is  $\{3, 7, 0\}$ , where the coefficient 3 occurs at time index  $-1$  and the coefficient 7 occurs at time index 0. The reverse is anticausal. The delayed reverse of  $\{0, 7, 3\}$  is the maximum-delay wavelet  $\{0, 3, 7\}$ , where the coefficient 3 occurs at time index 0 and the coefficient 7 occurs at time index 1.

An important type of wavelet is the causal all-pass wavelet  $p$ . A causal all-pass wavelet has an amplitude spectrum equal to unity for all frequencies. A causal all-pass wavelet is the impulse response of a recursive filter with transfer function

$$P(Z) = \frac{A^{\text{DR}}(Z)}{A(Z)}$$

where  $A(Z)$  is the  $Z$  transform of a finite-length minimum-delay wavelet  $a$ , and  $A^{\text{DR}}(Z)$  is the  $Z$  transform of the delayed reverse  $a^{\text{DR}}$ . This delayed reverse is, of course, maximum-delay. Because a causal all-pass wavelet has a unit-amplitude spectrum, its inverse is equal to its reverse:  $p^{-1} = p^{\text{R}}$ . The inverse is anticausal.

Generally a causal all-pass wavelet has infinite length. However, in two special cases the causal all-pass wavelet reduces to a finite-length wavelet. In the first special case,  $A(Z)$  is a constant. As a result the transfer function of the causal all-pass wavelet is equal to one, so the causal all-pass wavelet is the unit spike  $\{1, 0, 0, \dots\}$  where the 1 occurs at time index 0. Such a causal all-pass wavelet is called *trivial* because the unit spike convolved with any signal does not change the signal. In the second special case,  $A^{\text{DR}}(Z) = Z^n$ , where  $n$  is a positive integer. In this case,  $P(Z) = Z^n$ , so the causal all-pass wavelet produces a pure delay of  $n$  time units.

Let  $w_{\text{M}}$  be the minimum-phase wavelet with the same amplitude spectrum as the causal wavelet  $w$ . Then  $w_{\text{M}}$  is called the minimum-phase counterpart of  $w$ . The canonical representation states that any causal wavelet  $w$  can be represented as the convolution of its minimum-phase counterpart  $w_{\text{M}}$  and a causal all-pass wavelet  $p$ ; that is,

$$w = w_{\text{M}} * p$$

Because the inverse of a minimum-phase wavelet is minimum-phase, it follows that  $w_{\text{M}}^{-1}$  is minimum-phase, and hence causal. From the canonical representation, it is seen that the inverse wavelet is given by

$$w^{-1} = w_{\text{M}}^{-1} * p^{-1}$$

Two cases can occur. In the first case, the causal wavelet  $w$  is itself minimum-phase. Then the causal all-pass wavelet is trivial, so the inverse wavelet is simply  $w^{-1} = w_{\text{M}}^{-1}$ . In this case, the inverse wavelet is minimum-phase and causal. In the second case, the causal wavelet  $w$  is not minimum-phase. Then the causal all-pass wavelet  $p$  is not trivial, so its in-

verse  $p^{-1} = p^{\text{R}}$  is anticausal. In this case, the inverse wavelet  $w^{-1}$  is a noncausal (two-sided) wavelet.

J. P. Morlet, a French exploration geophysicist, was dealing with the Gabor transform. This transform covers the time-frequency plane with uniform cells, and associates each cell with a wavelet of invariant envelope but with a carrier of variable frequency. Morlet perceived that it was the wavelet shape that must be invariant to give uniform resolution in the entire plane. To do this, Morlet adapted the sampling rate to the frequency, thereby creating a changing time scale producing a stretching of the wavelet. He called this technique the *cycle-octave transform*. Later Grossman and Morlet (7) used the expression "wavelets of constant shape" so the cycle-octave transform became universally known as the *wavelet transform*. Even though the word *wavelet* was established in geophysics, the word caught on in mathematics and is now firmly entrenched.

## SPECTRAL ANALYSIS

Spectral analysis plays an important role in signal processing (8). A digital signal is obtained by sampling a continuous-time signal at equally-spaced times. The time-spacing of the sample is  $\Delta t$ . The equation connecting the discrete time integer  $i$  of the digital signal with the true time scale  $t$  of the continuous-time signal is  $t = i \Delta t$ . The Nyquist frequency is defined as

$$f_{\text{N}} = \frac{1}{2 \Delta t}$$

For example, in seismic work the value of  $\Delta t$  might be 4 ms, in which case the Nyquist frequency would be 125 Hz. The spectrum of the finite-length wavelet  $\{a_0, a_1, \dots, a_m\}$  is defined as the discrete Fourier transform

$$\begin{aligned} A(f) &= a_0 + a_1 e^{2\pi j f \Delta t} + a_2 e^{2\pi j f^2 \Delta t} + \dots + a_m e^{2\pi j f^m \Delta t} \\ &= |A(f)| e^{\phi(f)} \end{aligned}$$

In regard to the Fourier transform, the convention used here is the one common in the physical sciences. (In electrical engineering, the sign of the exponent is reversed.) The spectrum is obtained from the transfer function  $A(Z)$  by replacing  $Z$  with  $e^{2\pi j f \Delta t}$ . The use of the same symbol  $A$  for both the transfer function and the spectrum is commonplace. The magnitude  $|A(f)|$  is called the amplitude spectrum, and the angle  $\phi(f)$  is called the phase spectrum. The energy spectrum is the square of the amplitude spectrum. The energy spectrum is the discrete Fourier transform of the autocorrelation.

The *phase jump* is defined as the total phase shift over the Nyquist range; that is, the phase jump is  $\phi(f_{\text{N}}) - \phi(-f_{\text{N}})$ . A causal wavelet is *minimum-phase* if and only if its phase jump is zero. An  $(n + 1)$ -length causal wavelet is *maximum-phase* if and only if its phase jump is  $n\pi$ . If its phase jump is between the limits of 0 and  $n\pi$ , the wavelet is *mixed-phase*. The terms minimum-phase, mixed-phase, and maximum-phase apply only to causal wavelets.

The phase spectrum of a minimum-phase wavelet is uniquely derivable from its amplitude spectrum. This result means that the coefficients of a minimum-phase wavelet can be uniquely determined from knowledge of its amplitude spec-

trum. Equivalently, the coefficients of a minimum-phase wavelet can be uniquely determined from knowledge of its autocorrelation.

### THE STRATIFIED OR LAYERED MODEL

The first step in seismic signal processing is the construction of a model that can be used to explain the propagation of seismic waves. The most valuable models are three-dimensional (3-D). Such models have to be determined empirically, as the mathematics of a theoretical 3-D model is much too involved to obtain closed solutions except in the simplest cases. Since the most pronounced variations in the earth layering are along the vertical scale, a 1-D vertical model is often used. The foremost 1-D model, namely, the so-called stratified or layered earth model, is mathematically identical to the lattice model for electric transmission lines. The model is also mathematically identical both to the acoustic tube model used in speech processing and to the thin-film model used in optics (9). See Fig. 1.

In this model, the earth is mathematically sliced into many thin horizontal layers normal to the vertical  $z$  direction. This theoretical division produces a stratified medium characterized by the interfaces between the layers. The time unit is chosen to be the time spacing  $\Delta t$  on the seismic trace. The thickness of each layer is chosen so that the one-way travel time is one-half the time unit. The reason for this choice of thickness is so that the two-way travel time (downward time plus upward time) in each layer will be equal to one unit. Each interface separating two adjacent layers with different impedances has a nonzero reflection coefficient. The greater the impedance contrast between the two adjacent layers, the greater is the magnitude of the reflection coefficient. For computation, the wave motion is digitized so that a signal becomes a discrete sequence (that is, a time series with values separated by the given time unit). As a matter of convenience, the amplitude of a signal is measured in terms of a unit that represents the square root of energy. In this way, the sum of squares of the coefficients of a wavelet gives the energy of

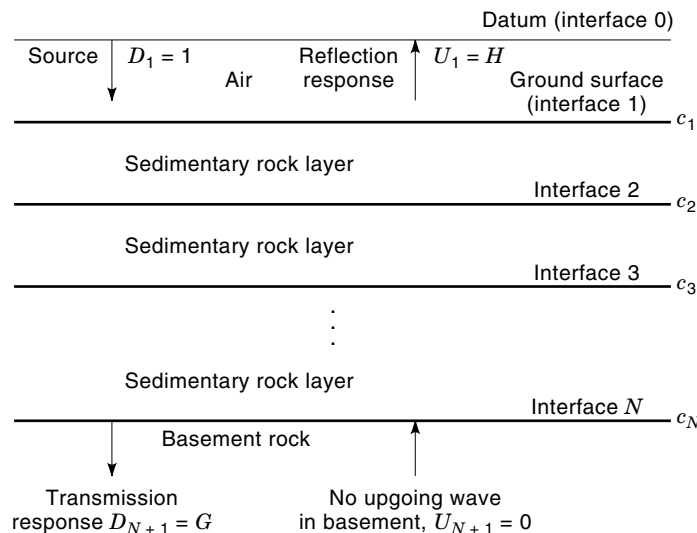


Figure 1. The stratified or layered earth model.

the wavelet. Also, in the basic model treated here there is no dissipation of kinetic energy into heat. Thus all the source energy imparted to the body can be accounted for, over time, in terms of the resulting elastic wave motion.

In the stratified model the boundary layers are the air (on the top) and the basement rock (on the bottom). Let  $N$  be the number of interfaces, with interface 1 the ground surface and interface  $N$  the deepest interface. A plane wave is the simplest form of wave motion. We consider plane-wave motion traveling normal to the interfaces, that is, waves traveling up and down in the vertical  $z$  direction. A pulse normally incident on interface  $i$  is divided into a reflected pulse and a transmitted pulse. Energy is conserved. As a consequence, the magnitude of the reflection coefficient  $c_i$  must be less than one. The magnitude of the reflection coefficient does not depend upon the direction in which the pulse travels through the interface, but the sign of the reflection coefficient does. For a given interface, the reflection coefficient for an upgoing pulse is the negative of the reflection coefficient for a downgoing pulse. The sequence  $c = \{c_1, c_2, \dots, c_N\}$  of the downgoing reflection coefficients is called the reflectivity function or simply the reflectivity. The reflectivity represents the internal structure of the earth. The reflectivity is an unknown quantity in the remote detection problem faced in seismic prospecting.

The transmission coefficient  $\tau_i$  and the reflection coefficient  $c_i$  for a given interface satisfy a Pythagorean relationship. Thus the transmission coefficient is given by  $\tau_i = \sqrt{1 - c_i^2}$ . It is convenient to choose the positive square root for both the case of a downgoing incident pulse and the case of an upgoing incident pulse. As a result, the transmission coefficient for an interface is the same in either direction. The one-way transmission factor through  $k$  interfaces (downward, or equivalently upward) is defined as

$$\sigma_k = \sqrt{(1 - c_1^2)(1 - c_2^2) \cdots (1 - c_k^2)}$$

for  $k = 1, 2, \dots, N$  and  $\sigma_0 = 1$ . The one-way transmission factor  $\sigma_k$  lies between zero and one.

Let  $D_k(Z)$  and  $U_k(Z)$  be respectively the transfer functions of the downgoing wave and the upgoing wave at a point just below interface  $k - 1$ . The Lorentz transform between two adjacent layers can be written in matrix form as

$$\begin{bmatrix} D_{k+1} \\ U_{k+1} \end{bmatrix} = \frac{Z^{-1/2}}{\tau_k} \begin{bmatrix} Z & -c_k \\ -c_k Z & 1 \end{bmatrix} \begin{bmatrix} D_k \\ U_k \end{bmatrix}$$

Define the fundamental polynomials  $P_k(Z)$  and  $Q_k(Z)$  and their delayed reverses

$$P_k^{DR}(Z) = Z^k P_k(Z^{-1})$$

$$Q_k^{DR}(Z) = Z^k Q_k(Z^{-1})$$

by the recursion (10)

$$\begin{bmatrix} P_k^{DR}(Z) & Q_k^{DR}(Z) \\ Q_k(Z) & P_k(Z) \end{bmatrix} = \begin{bmatrix} Z & -c_k \\ -c_k Z & 1 \end{bmatrix} \begin{bmatrix} P_{k-1}^{DR}(Z) & Q_{k-1}^{DR}(Z) \\ Q_{k-1}(Z) & P_{k-1}(Z) \end{bmatrix}$$

Note that the use of the symbol  $P$  to represent a fundamental polynomial is different from its use previously to represent a

causal all-pass filter. The recursion can be written as

$$\begin{aligned} P_k(Z) &= P_{k-1}(Z) - c_k Z Q_{k-1}^{\text{DR}}(Z) \\ Q_k(Z) &= Q_{k-1}(Z) - c_k Z P_{k-1}^{\text{DR}}(Z) \end{aligned}$$

As initial conditions, set  $P_0(Z) = 1$  and  $Q_0(Z) = 0$ . The sequence of fundamental polynomials  $P_k(Z)$  and  $Q_k(Z)$  for  $k = 1, 2, \dots, N$  characterize the stratified system. Although  $P_k(Z)$  is actually a polynomial of degree  $k - 1$ , it is treated as if it were a polynomial of degree  $k$  with last coefficient 0. The first coefficient of  $Q_k(Z)$  is zero.

### Dynamic Convolution and Dynamic Deconvolution

Because energy absorption effects are neglected, the layered system represents a lossless system in which energy leaves the system only by net transmission downward into the basement rock or net reflection upward into the air. For convenience, the source and receiver are mathematically placed on a datum, called interface 0, which is one-half time unit above the surface (which is interface 1). If the input is a unit downgoing spike (i.e., a unit impulse), then the transmitted wave is called the transmission impulse response, and the reflected wave is called the reflection impulse response. The reflection impulse response is denoted by

$$h = \{h_1, h_2, h_3, \dots\}$$

Note that the first nonzero coefficient  $h_1$  occurs at time index 1, because it takes one time unit for the pulse to travel from the source on the datum to the surface of the earth and back to the receiver on the datum.

Consider the forward problem. The initial conditions are: (1) the source is a downgoing unit spike (an impulsive unit source) initiated at time 0 on the datum, so  $D_1(Z) = 1$ , and (2) there is no upgoing wave motion in the basement, so  $U_{N+1}(Z) = 0$ . It is required to find the transfer function  $G(Z) = D_{N+1}(Z)$  of the transmission impulse response and the transfer function  $H(Z) = U_1(Z)$  of the reflection impulse response. Sequential application of the Lorentz transformation gives

$$\begin{bmatrix} G(Z) \\ 0 \end{bmatrix} = \frac{Z^{-N/2}}{\sigma_N} \begin{bmatrix} P_N^{\text{DR}}(Z) & Q_N^{\text{DR}}(Z) \\ Q_N(Z) & P_N(Z) \end{bmatrix} \begin{bmatrix} 1 \\ H(Z) \end{bmatrix}$$

The solution of these equations gives the transfer function of the transmission impulse response as

$$G(Z) = \frac{\sigma_N Z^{N/2}}{P_N(Z)}$$

and the transfer function of the reflection impulse response  $h$  as

$$H(Z) = \frac{-Q_N(Z)}{P_N(Z)}$$

Because physically the transmission impulse response is a causal transient time function, it follows that  $P_N(Z)$  is minimum phase. However, the minimum-phase property of  $P_N(Z)$  can also be established mathematically by using the fact that each reflection coefficient is less than one in magnitude.

An alternative expression for  $H(Z)$  can be found as follows. The reflection impulse response can be decomposed into a sum of components, each component uniquely associated with an interface. The wave motion that touches down at interface  $k$  but goes no deeper is the characteristic contribution of interface  $k$  to  $H(Z)$ . The expression for this contribution can be found by multiplying together the following five factors: (1) the factor  $\sigma_k Z^{k/2}/P_k(Z)$  for transmission from the source to a point just below interface  $k$ , (2) the factor  $1/\tau_k$  to back up to a point just above interface  $k$ , (3) the factor  $c_k$  to reflect off interface  $k$ , (4) the factor  $\sigma_{k-1} Z^{(k-1)/2}/P_{k-1}(Z)$  for transmission to a point just above interface 1, and (5) the factor  $Z^{1/2}$  for transmission to the datum. The final result of this multiplication is

$$\frac{\sigma_{k-1}^2 c_k Z^k}{P_{k-1}(Z) P_k(Z)}$$

This expression gives the contribution of interface  $k$  to the reflection impulse response. It shows that, for each constant  $c_k \sigma_{k-1}^2$  made up of the reflection coefficient of interface  $k$  multiplied by the two-way transmission factor through the interfaces above interface  $k$ , there is a wavelet  $w_k = \{w_{k,0}, w_{k,1}, w_{k,2}, \dots\}$  with  $Z$  transform

$$W_k(Z) = \frac{1}{P_{k-1}(Z) P_k(Z)}$$

This wavelet, which depends only upon reflection coefficients from the surface down to and including interface  $k$ , is called the dynamic wavelet for interface  $k$ . Each dynamic wavelet is minimum-phase. The sum of these contributions for all the interfaces gives the alternative expression

$$H(Z) = \sum_{k=1}^N \frac{\sigma_{k-1}^2 c_k Z^k}{P_{k-1}(Z) P_k(Z)}$$

for the transfer function of the reflection impulse response  $h = \{h_1, h_2, h_3, \dots\}$ . In the time domain the above expression for  $H(Z)$  gives the dynamic convolutional model

$$h_k = c_1 \sigma_0^2 w_{1,k-1} + c_2 \sigma_1^2 w_{2,k-2} + \dots + c_N \sigma_{N-1}^2 w_{N,k-N}$$

for  $k = 1, 2, 3, \dots$ . This model displays the reflection impulse response as the sum of the delayed dynamic wavelets, each weighted by the product of its reflection coefficient and its two-way transmission factor. The delay comes from the factor  $Z^k$  in the transfer function  $H(Z)$ .

Dynamic convolution, which represents the forward problem, involves finding the reflection impulse response  $h$  from the reflectivity  $c$ . Dynamic deconvolution, which represents the inverse problem, involves finding the reflectivity  $c$  from the reflection impulse response  $h$ . Details are given in Ref. 8.

### Small Reflection Coefficients

A reflection coefficient can be positive or negative, but its magnitude must be less than one. Generally, the reflection coefficients encountered in seismic prospecting are much less than one. Whenever the reflection coefficients cluster around the mean value of zero, they are considered small. In the case of small reflection coefficients, the symbol  $\epsilon_i$  is often used in-

stead of the symbol  $c_i$ . It is said that the reflection coefficients  $\epsilon_1, \epsilon_2, \dots, \epsilon_N$  are *small* provided that two-way transmission factor  $\sigma_N^2$  is equal to one or is nearly equal to one. The concept of smallness is made more precise as follows. If the magnitude of  $\epsilon_i$  is small, then  $\epsilon_i^2$  is very small, so the logarithm of  $\sigma_N^2$  has the approximation

$$\log \sigma_N^2 = \sum_{i=1}^N \log(1 - \epsilon_i^2) \approx - \sum_{i=1}^N \epsilon_i^2$$

The root-mean-square (rms) reflection coefficient is defined as

$$\epsilon_{\text{rms}} = \sqrt{\frac{\epsilon_1^2 + \epsilon_2^2 + \dots + \epsilon_N^2}{N}}$$

so the two-way transmission factor has the approximate formula

$$\sigma_N^2 = \exp(-N\epsilon_{\text{rms}}^2)$$

A small reflection coefficient series can be defined as a series for which  $N\epsilon_{\text{rms}}^2 \approx 0$ . In such a case,  $\sigma_N^2$  is almost one, so the transmission loss is small.

For example, if  $\epsilon_{\text{rms}} = 0.05$  and  $N = 100$  layers, then the two-way transmission factor would be approximately

$$\sigma_N^2 = \exp[-100(0.0025)] = 0.78$$

That is, an initial unit spike (amplitude 1), after traveling down and back up on a direct path through the 100 interfaces, would be received as a spike of 0.78, which represents a loss of  $1 - 0.78 = 0.22$  or about 22%. For  $\epsilon_{\text{rms}} = 0.01$ , the two-way transmission factor for 100 layers is 0.99, which is a small loss of only 1%. However, for  $\epsilon_{\text{rms}} = 0.01$  and  $N = 1000$  layers, the factor is 0.90, so 10% is lost on the direct transmission path down and back up.

Clearly, then, the definition of a small reflection coefficient series depends upon the number of interfaces; a larger number of interfaces requires a smaller rms reflection coefficient. Thus, considering a sedimentary basin in terms of a few major layers (representing the coarsest division into geologic epochs), there are quite small transmission losses for even large values of  $\epsilon_{\text{rms}}$ . In contrast, the transmission loss through a large number of interfaces can be significant. A large number of individually insignificant interfaces can have at least as great an effect as a few major ones. And, since the earth's stratification can be very fine, careful geologic study and analysis are necessary before the true significance of transmission losses can be assessed. This is an unexpectedly difficult problem. It is clear that, over a given up-and-down path in the earth, there must be a definite and altogether real transmission loss, but the obvious way to measure it from a velocity log computed from downhole data obtained from an existing oil well presents many difficulties.

Small reflection coefficients are important because an essential mathematical simplification occurs in that case. The simplification is expressed as follows. If a layered system of  $N$  interfaces has reflection coefficients  $\epsilon = (\epsilon_1, \epsilon_2, \dots, \epsilon_N)$  that are small in magnitude, then the fundamental polynomials are approximately given by the expressions

$$P_N(Z) \approx 1 + \gamma_1 Z + \gamma_2 Z^2 + \dots + \gamma_{N-1} Z^{N-1}$$

$$Q_N(Z) \approx -\epsilon_1 Z - \epsilon_2 Z^2 - \dots - \epsilon_N Z^N$$

where  $\gamma_i$  is the autocorrelation coefficient

$$\gamma_i = \sum_{j=1}^{N-i} \epsilon_{j+i} \epsilon_j \quad \text{for } i = 1, 2, \dots, N-1$$

of the reflection coefficient sequence. These equations show that for small reflection coefficients, the only two mathematical entities that enter into the layered-earth model are the reflection coefficient sequence itself and its autocorrelation. Thus in the case of small reflection coefficients, the layered-earth model does not require any higher-order function of the reflection coefficients.

Using the above equations, the reflection impulse response in the case of small reflection coefficients becomes

$$H(Z) = \frac{\epsilon_1 Z + \epsilon_2 Z^2 + \dots + \epsilon_N Z^N}{P_N(Z)}$$

When the reflection coefficients are both small and random, then the autocorrelation coefficients  $\gamma_i$  for  $i = 1, 2, \dots, N-1$  are approximately zero. In such a case,  $P_N(Z) \approx 1$ , so the transmission impulse response is

$$G(Z) = \frac{\sigma_N Z^{N/2}}{P_N(Z)} \approx \sigma_N Z^{N/2}$$

and the reflection impulse response is

$$H(Z) = \epsilon_1 Z + \epsilon_2 Z^2 + \dots + \epsilon_N Z^N$$

Thus, in the case of a small white reflectivity, transmission merely produces a scalar attenuation  $\sigma_N$  and a delay of  $N/2$ , whereas reflection simply produces the reflection coefficient sequence itself; that is,  $h = \{\epsilon_1, \epsilon_2, \dots, \epsilon_N\}$ . In other words, in the case of a small white reflectivity, the reflection impulse response consists of only primary reflections with no transmission losses and no multiple reflections. It follows that if an arbitrary wavelet is the input to a system with small white reflectivity, the same wavelet delayed by  $N/2$  and multiplied by the scalar  $\sigma_N$  will be the transmitted output, and the wavelet convolved with the reflectivity will be the reflected output. Therefore, a small white reflectivity passes a wavelet in transmission with no change in shape and passes a wavelet in reflection as a linear time-invariant filter with impulse response  $\epsilon = \{\epsilon_1, \epsilon_2, \dots, \epsilon_N\}$ .

The time-invariant seismic convolutional model (discussed below) is based upon this central result. A small white reflectivity acts as an ideal window, producing perfect transmission and perfect primary reflections. A multiple reflection represents seismic energy that has been reflected more than once. If we strictly adhere to this definition, then virtually all seismic energy involves multiples, and primary energy that has been reflected only once is hardly observable. However, a small white reflectivity produces no visible multiple reflections on the seismic trace. Instead, all the multiple energy goes to reinforcing the primary reflections.

An explanation can now be given why, before the advent of digital signal processing, the seismic method was successful in some areas when just the raw records were interpreted. The reason is that these good areas had, for the most part, small white reflectivities. In those prospects where the reflectivity

tivities were interlaced with large or unusual patterns of reflection coefficients, NG records were obtained. These NG records were fraught with strong multiple reflections and other types of noise that obscured the primary reflections, thereby making the records unintelligible for direct visual inspection. The digital method of predictive deconvolution, by removing these strong multiples, opened up these NG prospects to exploration.

### Time-Invariant Convolutional Model

The stratified model can be used to examine the case of water reverberations. The water–air interface is a strong reflector, with reflection coefficient  $c_1 = a$  close to unity. The water–bottom interface is also a strong reflector, with reflection coefficient  $c_{T+1} = b$ . Suppose that the interfaces below the water bottom have small white reflection coefficients  $\{c_{T+2}, c_{T+2}, \dots, c_N\} = \{\epsilon_{T+2}, \epsilon_{T+2}, \dots, \epsilon_N\}$ . The water layer acts as an imperfect energy trap in which a seismic pulse is successively reflected between its two interfaces. Seismic energy from the source first encounters the water layer on its way downward. The transmitted energy proceeds towards the deep interfaces, where it is reflected. Upon reflection, the energy returns in the upward direction, where it again encounters the water layer. The multiple reflections within the water layer appear on the seismic trace as reverberations, which obscure the reflections from the deep horizons.

The two-way travel-time parameter in the water layer, an integer denoted by  $T$ , is called the cycle time of the reverberation. Suppose that  $T = 3$ . Then the reflectivity can be written as

$$c = \{a, 0, 0, b, \epsilon_5, \epsilon_6, \dots, \epsilon_N\}$$

For interfaces from the surface (interface 1) down through the water bottom (interface 4), the dynamic wavelets are

$$w_1 = w_2 = w_3 = \{1, 0, 0, \dots\}$$

and  $w_4 = \{1, 0, 0, -ab, 0, 0, a^2b^2, 0, 0, -a^3b^3, \dots\}$

The wavelet  $w_4$  represents the multiple reflections from the water bottom. Because the reflection coefficients are small and random for the deeper interfaces, the dynamic wavelets for the deeper interfaces 5, 6, . . . ,  $N$  are approximately all equal to the so-called multiple wavelet

$$m = \{1, 0, 0, -2ab, 0, 0, 3a^2b^2, 0, 0, -4a^3b^3, \dots\}$$

The wavelet  $m$ , as given here, is the dynamic wavelet obtained for each of these deeper interfaces by setting  $\epsilon_5 = \epsilon_6 = \dots = \epsilon_N = 0$ . The multiple wavelet  $m$  in the present case represents the water reverberations. The dynamic convolutional model becomes approximately

$$h_k = aw_{1,k-1} + b(1 - a^2)w_{4,k-4} + (1 - a^2)(1 - b^2) \sum_{i=5}^N \epsilon_i m_{k-i}$$

It is seen that the last term is a time-invariant convolution. Thus the reflection impulse response for time indices beyond the arrival time of the water–bottom primary reflection is approximately given by the time-invariant convolutional model

$$h = (1 - a^2)(1 - b^2)m * \epsilon$$

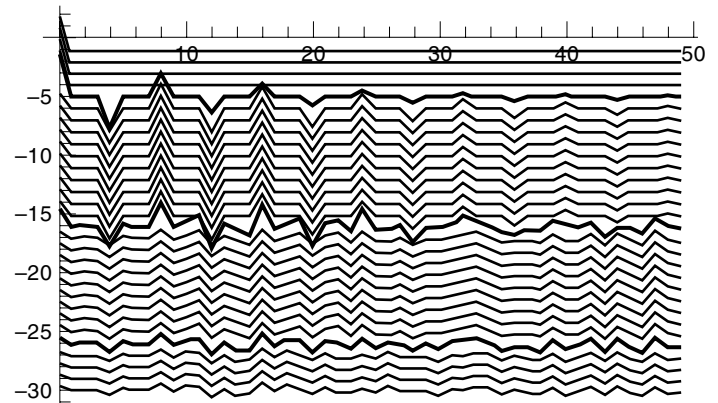


**Figure 2.** Dynamic wavelets for each interface with the water surface on top. The heavy lines show the dynamic wavelets for the major interfaces, and the light lines for the minor interfaces.

The inverse of the wavelet  $m$  is the minimum-delay dereverberation filter

$$m^{-1} = \{1, 0, 0, \dots, 0, 2ab, 0, 0, \dots, 0, a^2b^2\}$$

The convolution of  $m$  and  $m^{-1}$  gives a unit spike. The inverse filter  $m^{-1}$  when convolved with the trace eliminates the water-layer reverberations on the trace. The dereverberation filter  $m^{-1}$  can be determined by estimating three parameters—the reflection coefficients  $a$  and  $b$  at the surface and water bottom, respectively, and the discrete two-way travel-time parameter  $T$  in the water layer.

Physical parameters such as layer depths and reflection coefficients provide the required information to design the dereverberation filters. In contrast, an important strategic feature of predictive deconvolution (to be discussed below) is that dereverberation filters designed from the seismic data provide estimates of physical parameters such as layer depths and reflection coefficients. In this sense, the approach given in this section and the approach of predictive deconvolution are dual to each other with respect to petrophysical parameters versus seismic parameters. For example, using the layer depths and reflection coefficients computed from downhole information, the predictive deconvolution filter can be obtained as shown above. The same predictive deconvolution filter can be found independently from the seismic data, as shown in the next section, in the subsection on predictive deconvolution. These two versions of the filter can be used to tie the downhole data and the seismic data together. This dual approach is especially useful in the design of filters targeted to remove specific multiples.

Let us now give an example of the approach given here. The prospect is a marine area, with the reflection coefficient of the water surface equal to 0.9, the reflection coefficient of the water bottom (interface 5) equal to 0.8, and two major reflectors at depth, namely, interface 16 with reflection coefficient equal to  $-0.8$ , and interface 26 with reflection coefficient equal to 0.6. The water layer has no physical interfaces, so the dynamic wavelets in the water layer are merely spikes due to the impulsive source. Below the water bottom each interface has a dynamic wavelet. Now suppose that all the reflection coefficients between the major interfaces are small and white, lying in the range from  $-0.05$  to  $+0.05$ . These are minor reflection coefficients. The dynamic wavelets for this case are shown in the Fig. 2.

This figure demonstrates that the dynamic wavelets are approximately constant between the major reflectors. Thus between major reflectors the dynamic convolutional model reduces to the time-honored time-invariant model. The message is that deconvolution design gates should be chosen between major reflectors so that the time-invariant model approximately holds within each gate.

### GENERAL CONVOLUTIONAL MODEL

In an ideal seismic experiment, a impulsive source produces a reflection response. It is assumed that the seismic trace has been corrected for amplitude decay due to spherical spreading over the seismic time scale of interest (say from 0 to 6 s). However, in reality there are other effects that must be considered. One is the source wavelet, or source signature. Another is absorption, that is, the loss of elastic energy to heat. Also there are the modifications due to the receiving instruments. Under various approximations, serious or minor, the successive effects that produce the field seismic trace can be represented by a linear time-invariant convolutional model. The model states that the trace  $x$  is the convolution of the source signal  $s$ , the absorption response  $a$ , the receiver response  $r$ , and the reflection impulse response  $h$ ; that is,

$$x = s * a * r * h$$

The dynamic convolutional model displays the reflection impulse response  $h$  as a time-varying convolution of the reflectivity with causal dynamic wavelets. As shown previously, the reflection impulse response, within a time gate in which the reflectivity  $\epsilon$  is small and white, can be approximated by the linear time-invariant convolutional model

$$h = m * \epsilon$$

The multiple wavelet  $m$ , which includes such things as ghosts, reverberations, short-period multiples, and long-period multiples, is necessarily minimum-phase. Thus the trace  $x$  within the time gate has the time-invariant convolutional model

$$x = s * a * r * m * \epsilon$$

The convolutional model is important for the understanding of the seismic method. There has recently been a major resurgence in interest in the model because of its applicability in direct hydrocarbon detection, porosity mapping, and the dynamic removal of multiple reflections.

### Signature Deconvolution

The source signal  $s$  is called the signature. In an ideal situation the source signal would be chosen to be an impulsive signal, a Dirac delta function. In seismic exploration carried out on land, an explosion of dynamite can be used as the source signal. In such a case the signature starts out as a spike but soon loses high frequencies and broadens into a minimum-phase wavelet of some width. However, in many situations, nonimpulsive sources are used, such as a vibroseis on land or an air gun at sea. In such cases the shape of the signature is either measured directly or estimated. The pro-

cess of removing the known signature from the trace is called signature deconvolution. The resulting trace is called the *signature-deconvolved trace*. Signature deconvolution significantly reduces the complexity of reflection seismograms and makes them amenable to further analysis.

Signature deconvolution requires knowledge of the shape of the source signature. In marine seismic work the most popular source of energy is the air gun. Detailed knowledge of the signature of an air gun array can be obtained by direct measurement. Using this approach for every shot, however, can be expensive. As a result, computer models are often used to estimate the signatures. The basic building block of such a model is a description of the oscillating bubble produced by an air gun. The model must be able to cope with the interactions of the bubbles produced by the array, including the problem of heat transfer between the bubbles and the water. Because it is produced by a physical phenomenon, the signature must necessarily be a causal wavelet. However, because the bubble pulses of the air guns have large oscillations well after the time of initiation, the source signature is generally not minimum-phase.

The signature  $s$  has the canonical representation  $s = s_M * p$ , where  $s_M$  is the minimum-phase counterpart of  $s$  and where  $p$  is all-pass. In signature deconvolution, the inverse signature  $s^{-1}$  is applied to the trace in order to remove the signature. The result is the signature-deconvolved trace

$$y = s^{-1} * x = s^{-1} * s * a * r * h = a * r * h$$

The inverse signature can be obtained by least squares as follows. Design the least-squares causal inverse filter  $f$  by requiring that the causal signature  $s$  be the input to the filter and the zero-delay spike  $\delta$  be the desired output. The Toeplitz normal equations are

$$\sum_{j=0}^n f_j \phi_{ss}(i-j) = \phi_{ds}(i) \quad \text{for } i = 0, 1, \dots, n$$

where  $\phi_{ss}$  is the autocorrelation of  $s$  and  $\phi_{ds}$  is the crosscorrelation of  $\delta$  and  $s$ . The equation

$$\phi_{ds}(i) = \sum_k \delta_k s_{k-i} = s_{-i}$$

says that the crosscorrelation is simply the time reverse  $s^R$  of  $s$ . Thus the right-hand side of the normal equations is nonzero only for  $i = 0$ . Solution of the normal equations gives the least-squares inverse  $f$  of the signature. The least-squares inverse  $f$  is necessarily minimum-delay (11). Thus  $f$  is the required approximation to  $s_M^{-1}$ .

Next the causal all-pass wavelet  $p$  must be found. An approximation to  $p$  is obtained by convolving  $f$  with  $s$ . The inverse of  $p$  is the same as the reverse of  $p$ . The reverse is anticausal. Thus the convolution of  $f$  with  $p^R$  gives the required approximation to the inverse signature; that is,

$$f * p^R \approx s_M^{-1} * p^{-1} = s^{-1}$$

The inverse signature  $s^{-1}$  is two-sided. The convolution of  $s^{-1}$  with the trace  $x$  removes the signature wavelet to yield the required signature-deconvolved trace.



If the source signature cannot be conveniently measured, as on land, then various averaging techniques used on multifold data can be used to estimate and then remove the source signature. The same averaging techniques can also be used to remove the receiver response. The most successful of these averaging techniques is called *surface-consistent deconvolution*.

The receiving system includes the geophones or hydrophones, the amplifiers, and the modulation instruments, which place the digitized signal on tape. The individual contributions of each of the components can usually be either measured or estimated. All these components can be lumped together as the receiver response  $r$ . This response, in most cases, is minimum-phase. The receiver response can be removed by deconvolution in the same way as in signature deconvolution. Otherwise, a minimum-phase receiver response can be removed by predictive deconvolution as described in the next subsection.

In the propagation of seismic waves through the earth, some of the elastic energy of the waves is transformed into heat energy. This inelastic absorption of seismic energy has been a research topic for many years. Experimental results indicate that as a seismic wavelet travels through homogeneous rock, the wavelet systematically loses high frequencies to heat according to a filtering operation. This earth filter, called the absorption response, has magnitude spectrum approximately given by  $\exp(-2\pi \alpha f z)$ , where  $\alpha$  is a constant,  $f$  is the frequency, and  $z$  is the distance traveled. Moreover, the phase spectrum of the absorption response is minimum-phase. The absorption response can be removed by deconvolution. Absorption deconvolution consists in convolving the trace with the inverse  $\alpha^{-1}$  of the minimum-phase absorption response  $\alpha$ . Otherwise, the minimum-phase absorption response can be removed by predictive deconvolution as described in the following subsection.

### Predictive Deconvolution

The data processing method of prediction-error filtering is known as predictive deconvolution. The prediction-error filter is called the deconvolution filter; and the prediction-error series, the deconvolved signal. The filter is required to be causal. The deconvolved signal sharpens seismic resolution and provides an estimate of the reflectivity series. Depending upon the prediction distance  $\alpha$ , there are two types of predictive deconvolution filter. Spike deconvolution is the case when the prediction distance is equal to one time unit. Gap deconvolution is the case when the prediction distance is greater to one time unit. Ordinarily, one or the other of these two deconvolution processes is performed.

Predictive deconvolution is based upon the seismic convolutional model  $x = w_M * \epsilon$ . In the convolutional model we can think of the reflectivity  $\epsilon$  as the input, the wavelet  $w_M$  as the unit-impulse response function, and the trace  $x$  as the output. In this model, the reflectivity  $\epsilon$  is white. If no previous deconvolutions have been performed, the wavelet is

$$w_M = s * a * r * m$$

If signature deconvolution has been performed, then, of course, the signature component  $s$  is not present in the wavelet  $w_M$ , etc. For the application of predictive deconvolution it is assumed that all the components present in the wavelet

are minimum-delay, so the wavelet  $w_M$  itself is minimum-delay.

No other physical model in geophysics has come under such scrutiny as this convolutional model. No other construct has been more tested. Every single seismic trace for the past thirty years has been subjected to spike deconvolution and/or gap deconvolution. If this model did not hold, at least to a good approximation, these deconvolutions would have failed. The success of deconvolution depends upon this convolutional model.

The synthetic seismogram is an example of the direct use of the convolutional model. The reflectivity function is computed from downhole information obtained from an oil well. This reflectivity function as input is convolved with a seismic wavelet to produce the synthetic seismogram as output. The operation can be reversed. Thus the output can be spike-deconvolved to give the input. As such, spike deconvolution represents a type of seismic inversion. The deconvolution operation actually is done by convolution, that is, by the convolution of the deconvolution filter with the trace.

A given convolutional model is assumed to hold not for the entire trace but only within a specific time gate. In practice, several different gates are specified on a trace. If two adjacent gates do not overlap, the first deconvolution filter is applied down to the end of the first gate, then with decreasing linear taper down to the beginning of the second gate. If two adjacent gates overlap, the operator designed for the first gate is applied down to the beginning of the zone of overlap. The operator designed for the second gate is applied from beyond the zone of overlap. Within the zone of overlap, the filter is obtained as a time-varying weighted average of the filter designed in the first gate and the filter designed in the second gate. In the application of predictive deconvolution, it is assumed that within the time gate (1) the wavelet is unknown, but is minimum-delay, and (2) the frequency content of the reflectivity is completely white. The frequency content of the wavelet on the trace can be obtained by taking the autocorrelation of the trace. The reason is that the power spectrum of a white signal (i.e. the reflection coefficient series) is completely flat, so the colored frequency content of the wavelet is the same as that of the trace. In customary practice, the deconvolution filter is computed by the least-squares method, which leads to a set of Toeplitz normal equations. The known quantities in the Toeplitz normal equations are the autocorrelation coefficients of the trace. The deconvolution filter is found by solving the Toeplitz normal equations.

The purpose of spike deconvolution is to remove the wavelet  $w_M$  from the trace  $x$  while leaving the reflectivity  $\epsilon$  intact. The spike-deconvolution filter  $f$  is the least-squares inverse of the minimum-delay wavelet  $w_M$ ; that is,  $f \approx w_M^{-1}$ . When the spike deconvolution filter is convolved with the trace, the spike deconvolution filter is, in fact, convolved in turn with all of the wavelets that make up the trace. The operation converts each of these wavelets, as well as possible, into a spike, greatly improving seismic resolution. The amplitude of each spike is proportional to the corresponding reflection coefficient, and the sharpness will be a function of the frequency bandwidth. The spike can be no sharper than the best approximation possible with the available bandwidth. Thus the spike-deconvolved trace is approximately

$$y = f * x \approx w_M^{-1} * (w_M * \epsilon) \approx \epsilon$$

Spike deconvolution and gap deconvolution are intimately related. Let the gap-deconvolution filter (for prediction distance  $\alpha$ ) be denoted by  $g$ . The head  $h_\alpha$  is defined as the leading part of the minimum-delay wavelet  $w_M$ . More specifically, the head  $h_\alpha$  is defined as the first  $\alpha$  values of  $w_M$ . The gap-deconvolution filter  $g$  for a given value of  $\alpha$  is the convolution of the spike-deconvolution filter  $f$  with the head  $h_\alpha$ ; that is,  $g = f * h_\alpha$ . See Eq. 5.333 in Ref. 3. Because the spike-deconvolution filter  $f$  is necessarily minimum-delay, it follows that the gap-deconvolution filter  $g$  is minimum-delay if and only if the head  $h_\alpha$  is minimum-delay. The gap-deconvolved trace is approximately

$$z = g * x = (f * h_\alpha) * x = h_\alpha * (f * x) \approx h_\alpha * \epsilon$$

In conclusion, the spike-deconvolved trace  $y$  is (within the limits of least squares) the reflectivity series  $\epsilon$ , and the gap-deconvolved trace is (within the limits of least squares) the reflectivity series  $\epsilon$  smoothed by the head  $h_\alpha$ . For other methods of deconvolution, see Ref. 12.

## SEISMIC MIGRATION

Deconvolution and other signal processing methods remove the effects of source, absorption, multiples, and receiver from the traces. A collection of seismic traces make up a seismic time section (signals as a function of time plotted against horizontal coordinates). The seismic time section must then be transformed into a spatial image of the subsurface. This process is called *migration* because events occurring in time are moved to their true spatial position. The resulting image is called the *migrated section*. The migrated section is a depth section (signals as a function of depth plotted against horizontal coordinates). In one form or another, migration reconstructs the image at any point within the earth by use of various approximations to the wave equation and/or the associated eikonal equation (13,14).

A hologram contains the whole message, or entire picture (15). In simple terms, holography represents a method of recording the interference pattern of an object on a plane (the hologram). Illumination of the hologram reveals the entire picture of the object in three-dimensional space. In principle, a seismic section is a hologram, and the migration process corresponds to the illumination of the hologram in order to produce the required image. A hologram is made by shining laser light at an object. Half of the laser beam never hits the object because it is reflected from a mirror placed in its path. This reflected light, called the reference beam, is directed to a photographic plate. The other half of the laser beam finds the object. Each point P of the object acts as a diffraction point and spreads light in all directions. The diffracted light from point P reaches every point on the undeveloped plate. When the two halves of the laser light meet at the plate, they interfere with each other. The resulting interference pattern is recorded on the plate.

When developed, the plate becomes the hologram. When a laser beam is later directed through the hologram (with the object removed), an virtual image of the object unfolds from the wave pattern and projects three-dimensionally in space. A viewer walking around this chimerical object sees its image from different perspectives, even as he or she would see the real object. The reason is that the whole object has been re-

corded at every point of the interference pattern on the hologram. A hologram is a two-dimensional photographic plate that allows us to see a faithful reproduction of a scene in three dimensions.

Cutting a piece from the hologram and sending the laser beam through the fragment also produces an image of the whole object, although this image may not be quite as sharp. Let us now discuss why that is so. Each diffraction point of the object sends out waves that reach every point on the hologram. As a result each point on the hologram contains a contribution from every point on the object. It follows that every point on the hologram contains the entire picture. Thus when either the entire hologram is illuminated, or just a section of it, we see the image of the entire object. However, the more points used on the hologram, the better the quality of the picture. The characteristic that each part of a hologram contains the entire picture has widespread implications in seismology.

In an ordinary camera a lens is used to form an image of the object on the plane of the photograph film. Light reflected from a given point on the object is directed by the lens to the corresponding point on the film. Thus there is a one-to-one relationship between points on the object plane and points on the photograph film. Moreover, all the light that reaches the film comes from the object. There is no secondary source as in the case of a hologram. Let us now compare the ordinary camera with holography. In making a hologram, no image-forming lens is used. Thus each point on the object diffracts light to every point on the hologram plate. Thus there is a one-to-many relationship between points on the object and the points on the hologram plate. Every part of the hologram plate is exposed to light diffracted from every part of the object. Moreover, the total light that reaches the hologram plate is made up of two parts, namely the part of the beam (the reference beam) that is reflected from the mirror and the part that is used to illuminate the object. These two parts produce the interference pattern recorded on the hologram.

Because vast amounts of information are recorded on a hologram, the film used for a hologram must have a resolving power much greater than ordinary fine-grain photographic film. The developed hologram contains the intensity of the reference beam modulated by waves from the object. If we look directly at a hologram, we see no recognizable image. The hologram is dark where the object wave and the reference wave arrive in phase, and light where they arrive out of phase. Thus the intensity of the hologram corresponds to the phase difference between the object waves and the reference waves, and is unaffected by a change in sign of that difference. A hologram is a photograph of microscopic interference fringes, and appears as a hodgepodge of whirly lines. When the hologram is placed in a beam of laser light (with the object gone) the light rays are bent by the hologram to produce rays identical to the original rays diffracted by the object. When viewed by the eye the bent (or diffracted) rays produce the same effect as the original diffracted rays. When we look through the hologram, we see a full, realistic, 3-D virtual image as if we were viewing the object through a window. When we move our eyes to look at the sides or bottom of the object, parallax is evident as in real life. The entire wave field on our side of the hologram has been reconstructed by the illumination of the hologram by the laser light. We see the object as a virtual image, even though the original object is no longer present.

### The Seismic Section as a Hologram

Consider now the problem of seismic exploration for petroleum. The way of carrying out a seismic survey is, of course, different from the way a hologram is made. In holography, electromagnetic (light) waves are used. In the seismic case, acoustic (sound) waves are used. The laser waves are extremely narrow-band, and are, in fact, almost pure sine waves. In contrast, seismic waves are broadband waves. An important feature of seismic exploration is that there is an absolute reference time (the time of the shot); this feature makes it unnecessary to use a reference beam as in holography. On the photographic plate making up the hologram, only the intensity pattern of the interference is recorded. In seismic exploration the whole interference pattern is recorded as time-varying signals (the seismic traces). In holography, the exterior of an opaque object is imaged. In seismology, the entire interior structure of the earth is imaged because solid rock is transparent to seismic waves.

Seismic surveys are taken on the surface of the earth in order to determine the underlying three-dimensional structure. The sources and receivers are at grid points on the surface of the earth, and correspond to the holographic plate. The reflecting horizons are the interfaces between the sedimentary rock layers within the earth. These reflecting horizons represent the geologic object to be imaged. Waves reflected from the subsurface structure are returned to the receiving instruments on the surface and recorded as traces. These traces make up the various seismic sections. The seismic sections are the counterpart of the developed holographic plate. In fact, the totality of seismic sections from a prospect is a hologram in the true meaning of the word.

In seismic exploration, the subsurface object (the geology) is made up of a collection of reflection surfaces. However, any surface can be approximated by a set of closely spaced points lying on the surface. Each point of the set acts as a point diffractor. That is, a reflector is nothing more than a continuous collection of diffraction points. Rays from a diffraction point reach all points on the earth's surface. The seismic travel-time curve for the rays from a point diffractor is called the diffraction curve. The diffraction curve is the seismic section (or hologram) for the point diffractor. See Fig. 3.

When the layers of sedimentary rock lying beneath the earth's surface are relatively flat and unexceptional, the seismic section can give a remarkably direct indication of the structural configuration. Because the depth that a wave penetrates and its travel time are related by the velocity of the traveling seismic waves, there is a correspondence between the depth axis and the time axis. Thus the recorded seismic data (the seismic section) as a function of horizontal coordinate and time give a rough picture of the cross section of the earth that is a function of horizontal coordinate and depth. In this sense the seismic section is like a picture, albeit distorted, of the subsurface geologic structure. In the same way, a hologram is a picture of the object, but it is so distorted that no sense can be made of it as such.

In the case of a complex subsurface structure, a seismic section can be misleading and hard to interpret geologically even when the record quality (such as the continuity of reflected events and the ratio of reflected signal to background noise) is excellent. When the underground structure shows large deviations from horizontal layering, the subsurface posi-

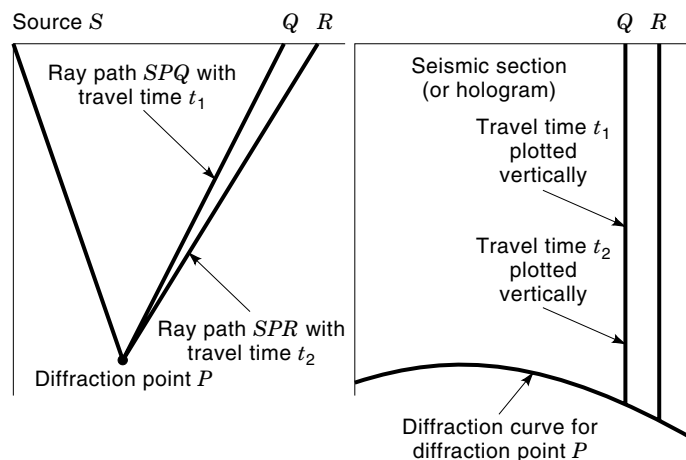


**Figure 3.** Recording a seismic section (or hologram). The returned signals from a diffraction point gives a hyperbolic-shaped diffraction curve. The geologic structure can be considered as composed of many diffraction points. The resulting seismic section is the superposition of all the diffraction curves.

tion of the reflecting point on an reflecting interface does not lie under the shot-receiver midpoint but is displaced to one side. The direction and magnitude of this displacement depend on the direction and magnitude of the dip of the reflecting interface. Therefore, the seismic section must be processed so that the event is moved (or migrated) to a position representing the correct spatial coordinates of the reflecting horizon. This processing technique, known as migration in exploration geophysics, is necessary in order to delineate correctly the oil-bearing structural traps (folds, faults, and domes). Migration is the seismic digital processing method that corresponds to the optical processing that takes place when the developed hologram is illuminated and viewed in order to yield the virtual image. In the true sense of the word, migration is the seismic counterpart of illuminating and viewing the developed hologram to bring out the virtual image in the eye of the observer. In the seismic case the virtual image, or migrated section, is a three-dimensional reconstruction in the computer of geologic objects that can be as much as 8 km below the surface of the earth.

### Migration as the Illumination and Viewing of a Hologram

The migration of seismic data is performed routinely in seismic processing regimes. Various techniques for migration are commonly available. The basic theory of migration can be explained in terms of diffraction curves and equitime curves. For purposes of exposition, it is easier to consider the case where the seismic data are taken along a single surface line, and to regard the underlying earth structure as two-dimensional. The two spatial dimensions are the horizontal coordinate  $x$  and the depth coordinate  $z$ . The variable  $x$  can take on any positive or negative value, but the variable  $z$  must be positive. Also, time  $t$  must be positive. Because  $z$  and  $t$  must be positive, there is a certain duality between them. There is nothing in our exposition that cannot be extended to three spatial dimensions; the extension is straightforward and involves no new principles.

The recorded seismic section forms the starting point for migration. The seismic section is produced by an seismic sur-

vey where each source–receiver pair produces a seismic trace. The totality of traces make up the seismic section. The wave equation describes the motion of the waves generated by the source. However, the seismic section does not correspond to a wave field resulting from any single experiment, because the sources are excited sequentially, not simultaneously. A seismic trace records the two-way travel times from a given surface source to all possible diffractors, and then back to a given surface receiver. The seismic sections contain the traces for all the source–receiver pairs used in the survey.

In seismic work the sources and receivers are at the surface of the earth and reflectors are at depth. A certain type of idealization deserves special study, namely, the case of a point reflector, which is also called a point diffractor. When such a point is illuminated by a surface source, it acts as a secondary source and hence sets off outgoing wave motion in all directions. Any reflecting surface may be considered as being made up of a dense set of point diffractors.

The time coordinate of each event on a trace gives the two-way travel time from the given source to an unknown diffraction point and back to the given receiver. Although the position of the diffraction point is unknown, it is known that it must lie somewhere on the curve defined by the given source, the given receiver, and the given two-way travel time. This curve, the locus of diffraction points that have the same travel time for the given source–receiver pair, is called the equitime curve. A equitime curve is defined by the source and receiver positions and the travel time of an event on the seismic trace recorded for that source–receiver pair. In equitime curve for each event on a seismic trace can be computed, and the actual diffraction point that produced that even must lie on that curve.

The migration problem can now be stated in the following terms. The equitime curves can be computed from the known data. The problem then is to determine where on that curve the true (geologic) diffraction point lies. The general idea of migration can be described as follows. Take an event on a trace in the seismic section, and throw it out onto its equitime curve in the spatial  $x$  and  $z$  dimensions. Keep repeating this process so as to obtain the totality of the equitime curves from each data point of every trace in the seismic section. Place all of these curves on the same graph. By the linear superposition principle, the result is the migrated section. That is, the migrated section is the superposition of all the equitime curves.

In the case of constant velocity, equitime curves are elliptical with the source and receiver as the foci. Generally, equitime curves are more complicated and must be computed according to a velocity function. A useful subsurface image is produced because of the constructive and destructive interference among the equitime curves. For example, equitime curves from neighboring traces will all intersect at a true reflection point, adding constructively to produce an image of the reflector in the form of a high-amplitude output. For a continuous geologic reflecting surface, equitime curves from adjacent traces are tangent to this surface and produce an image of the reflecting surface by constructive interference of overlapping portions of adjacent equitime curves. On the other hand, in subsurface regions without reflecting bodies, the equitime curves tend to cancel because of random interference effects.

In summary, migration takes the value of the trace at a given time and places this value evenly along the equitime curve specified by the given time. The migrated section is the sum of all the values on the equitime curves. See Fig. 4.

### Holistic Migration

The migration methods described to this point represent the way that migration is usually done (conventional migration). The use of the holographic principle in migration defines a new method of migration, appropriately called holistic migration, which is now coming into general use (16). Conventional migration fails to recognize that a seismic section is a hologram. A portion of a hologram can produce the same picture as the entire hologram. Suppose, for cost reasons, a survey must be laid out with detector spacing equal to two spatial units. It is a common assumption that this spacing of two units governs the Nyquist frequency, so the processing is done at a spacing of two units. Accordingly, by use of conventional migration, the resolution at depth is forced to be two spatial units. If it is desired that the resolution at depth be one spatial unit, then the common belief is that detectors must be laid out at a one-spatial-unit spacing. The cost of a 2-D survey with one-unit spacing is about twice the cost of a survey with two-unit spacing. Thus, according to commonly accepted beliefs, to double precision, one must double cost, or thereabouts.

That need not be so. One can double precision without any appreciable increase in cost. Alternatively, one can obtain the same precision at the half the cost. The way is to use holistic migration in seismic processing instead of conventional migration.

Observe that the seismic section from a two-unit sampling is a subset of the seismic section with one-unit sampling. That is, the two-unit section can be obtained from the one-unit sec-

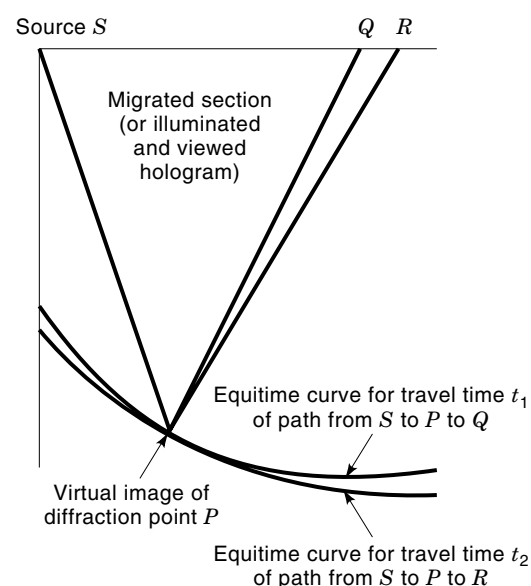


**Figure 4.** A representation of the process of migration. For each of traces  $Q$  and  $R$ , the amplitude value for the given travel time is mapped into the subsurface along the entire equitime curve, that is, the curve formed by the loci of points for which the travel time from source to diffraction point and back to receiver is constant. Constructive interference yields the image of the reflecting geologic interface.

tion by taking every other trace. In other words, the two-unit section (piece of the hologram) is obtained by cutting a piece from the one-unit section (the hologram). Because the piece of a hologram gives the same image (in all its detail) as the hologram, the same detailed subsurface image is produced by the seismic section with two-unit sampling as by the more costly seismic section with one-unit sampling.

The simplest possible example comparing conventional migration with holistic migration follows. The same seismic section is used for both conventional migration and holistic migration. The example is the case of a point diffractor as shown in Fig. 5. Diffractions differ from true reflections in that the energy from a shot returns from the vicinity of the point diffractor without appearing to obey the reflection law (incidence angle equals reflection angle). In the example shown in the figure, the given point diffractor falls through the cracks of conventional migration, but is easily found by holistic migration.

Any reflector may be considered as made up of a continuum of diffraction points lying on the locus of the reflector. As a result, any seismic section can be considered as the superposition of many such diffraction curves. Since the example shows that holistic migration works on such a curve, it follows that it works on the superposition of all the curves.

A hologram and a seismic section are the same in principle. When a hologram is illuminated or a seismic section is migrated, each depicts the entire image of the unattainable object. Moreover, any part of the hologram also depicts the entire image of the object. The same is true in the seismic case if conventional migration is replaced by holistic migration. Then any part of the seismic section produces the entire image of the subsurface.

Holistic methods allow wave-field images to achieve resolution beyond that predicted by conventional digital processing techniques. Suppose that a given number of shot points and detectors yields a certain resolution of the subsurface structure under conventional migration. Then one-half or one-

fourth as many shot points and detectors give the same resolution under holistic migration. The image may not be quite as clear, but the same fine structure is present. In this way, the number of shot points and detectors is greatly reduced without adversely affecting the results. Because the cost of a seismic survey depends directly upon the number of shot points and detectors used, the holistic method reduces the cost of a 3-D seismic survey greatly, often to one-fourth the previous cost or less. The fine details in geologic structure that fall through the cracks in conventional processing are captured in holistic processing.

## VELOCITY ANALYSIS AND TOMOGRAPHY

In reflection seismology, there are two equally important quantities: time of reflected events and velocity. With a knowledge of these quantities, the depth to the reflecting horizons can be found. Seismic waves travel with a velocity that is very much dependent on the medium. The assumption that the velocity is the same for two different forms of the same type of rock, such as two different sandstone formations, is generally not valid. The seismic wave velocity in various types of sandstone can vary over a wide range. Each new rock stratum encountered by the seismic waves has its own characteristic velocity and it is a challenge to the geophysicist to determine this velocity. Generally, velocity increases with depth, although occasionally there may be layers in which a decrease in velocity occurs. Seismic-processing methods must take into account that the velocity changes as the waves travel through the earth. Because velocity depends upon the position of the wave in the volume of the earth, a velocity function must be determined. If  $x$  and  $y$  are the horizontal dimensions, and  $z$  the vertical dimension, then  $v(z)$  denotes a velocity function in one dimension,  $v(x, z)$  in two dimensions, and  $v(x, y, z)$  in three dimensions.

*Velocity estimation* refers to finding empirical values for the velocity function. One method of measuring the velocity function  $v(z)$  is by use of an existing oil well. A continuous velocity log (CVL) is an instrument made up of a seismic pulse generator with two attached detectors that are a fixed distance apart. This fixed distance is only a few feet. As the instrument is gradually pulled up the well, the changes in transit time across the fixed distance between the two detectors are recorded as a continuous curve, known as the sonic log. The velocities determined by the CVLs are reasonably representative of the velocities of seismic waves through the corresponding formations, except under circumstances such as the case of the invasion of a porous formation by drilling fluid, so the velocity is not representative of the true formation velocity, and the case in which the hole diameter is very large or very irregular.

In many cases, it is necessary to estimate the velocity by measurements confined to the surface of the earth, since oil wells are available only in old prospects. Therefore, the actual seismic data must be used to estimate velocity. Velocity can be estimated by considering the time differentials of the same event received by a lateral array of detectors. Any such estimate always depends on a *ceteris paribus* (other things being equal) assumption. Computers can determine velocities by carrying out calculations based on many intricate time-distance relationships, and the results can present empirical

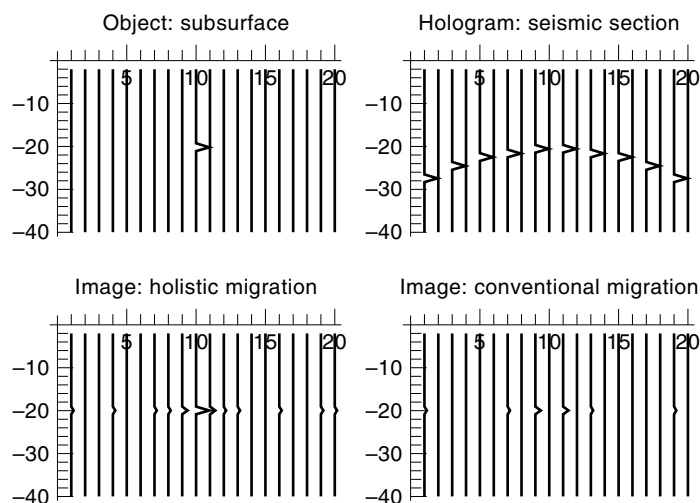


**Figure 5.** The object is a point diffractor as shown in the upper left diagram. The seismic section with every other trace missing is shown in the upper right diagram. Two methods of migration are applied to the seismic section. Holistic migration (lower left diagram) is successful in detecting the point diffractor, whereas conventional migration (lower right diagram) is not.

velocity as a function of travel time (or depth) in a display called a *velocity spectrum*. The empirical velocity so determined is called *stacking velocity*, and the problem is to relate this empirical quantity to a mathematical expression from which the thicknesses and velocities of the subsurface layers can be extracted (17).

In the past fifteen years travel-time tomography has been used as a general method for seismic velocity analysis (18,19). Seismic tomography can provide a means for velocity estimation in the case of either borehole data or surface reflection data. The goal of tomography is the imaging of material properties by using observations of wavefields which have passed through the body. The tomography method can be applied to the estimation of seismic velocities from travel-time information by means of three steps.

The first step is the data-gathering step in which seismic travel times for various source/receiver positions are measured. This procedure is time-consuming in that a geophysicist must often manually pick a multitude of events from the seismic data in order to determine the required travel times. For well-behaved seismic data, computer tracking programs can be used to make the picks automatically, thereby greatly decreasing the effort expended by the geophysicist. However, even with good data, the travel times resulting from automatic picking programs have to be visually inspected for quality control.

The second step is the modeling step in which seismic ray tracing methods are used in conjunction with a velocity model. The velocity model is used to find expressions for the travel times, the so-called travel-time equations. The subsurface is divided into cells for which a given velocity configuration is assigned. This velocity model allows velocity gradients in both the horizontal and vertical directions. Ray tracing methods that obey Snell's law are used so that the raypaths are correctly curved. The slowness (or reciprocal velocity) is used rather than velocity. The travel time in each cell is equal to the product of distance times slowness. A travel-time equation expresses the travel time for a raypath as the sum of such products for the cells traversed. The system of travel-time equations for all the raypaths is linear in slowness for the special case of straight raypaths. However, generally the raypaths curve according to Snell's law. As a result the distance values are themselves functions of slowness. In such cases, the system of travel-time equations is nonlinear.

The third step is a nonlinear iterative improvement method. In each iteration, the set of picked travel times obtained from the seismic data is matched to the computed travel times obtained from the travel-time equations. The travel-time equations require a velocity or slowness model. This velocity model starts with an initial best guess. For each iteration, the error between the two sets of travel times is used to update the velocity model. That is, the slowness vector is adjusted in each iteration so as to make the travel times given by the model agree more closely with the picked travel times. The iteration terminates when the agreement is deemed satisfactory. The result is the final velocity model.

Transmission tomography involves the modeling of rays which are transmitted without reflection from a known source position to a known receiver position. Transmission tomography can be used either in cross-borehole profiling or in vertical seismic profiling (VSP). In the cross-borehole case the sources are in one borehole and the receivers in another bore-

hole. In the VSP case the sources are on the earth's surface and the receivers are in the borehole.

Reflection tomography involves two-way transmission. The seismic waves from a surface source propagate to an interface where they are reflected. Then the waves propagate back upward to receivers on the surface. Because of the problem of defining the reflector position, reflection tomography is more difficult to apply than transmission tomography. In reflection tomography the ray-traced travel times of the model are matched to the picked travel times. The result of this iterative improvement method is an estimate of the interval velocities. Such velocity estimates are required to produce reliable images by seismic migration. In this sense, tomography and migration are complementary processes. In order to do tomography, a good depth image depicting the horizons (reflectors) is needed. A reliable depth image can be obtained by migration. The output of tomography is a reliable velocity model. In order to do migration, a reliable velocity model is needed. A reliable velocity model can be obtained by tomography. The output of migration is a reliable depth image depicting the horizons (reflectors). Consequently the processes of tomography and migration can be used iteratively in order to produce both reliable velocity models and reliable depth images.

## SEISMIC DATA INTERPRETATION

The subsurface structure and stratigraphy of the earth represent an unknown. The known information is in the form of the received (raw) seismic traces. These traces are a record of the seismic wavefield (the motion of seismic waves) at the surface of the earth. The geophysicist is faced with an inverse problem in which the received wavefield must be converted into a picture of the subsurface. The purpose of seismic processing is to solve the inverse problem so as to reveal the shape and properties of the geologic bodies that produced the recorded traces. Velocity analysis, deconvolution, and migration are the principal tools used in this task. The final result of seismic processing is an image of the underground structure and stratigraphy. In a three-dimensional (3-D) survey, the final image is a picture of the subterranean volume of the earth. The horizontal dimensions are north and east, and the vertical dimension is depth. In those cases for which a time-to-depth conversion has not been made, the vertical dimension would instead be time. Whereas the recorded (raw) seismic data represent a wavefield, the processed seismic data should represent a geologic image, or picture, of the subterranean earth. This picture stands by itself, apart from its wave-motion origin. The many faceted features of the picture are intended to reveal not only the subsurface geologic structure but also important clues as to the stratigraphy.

At this point, a word about the terminology is in order. A geologic image, within the computer, is in the form of an array of data points. The array is two dimensional for a 2-D image and three dimensional for a 3-D image. However, for historical reasons, the old terminology of trace (which originally was used only for wave motion) is still used in geophysics as a descriptive term in the makeup of an image. Thus, in current terminology, a geologic image is made up of individual traces extending in depth (or, equivalently, in travel time), one trace for each surface point. Traces occurring in a geologic image represent geology and not the wave motion

from which they were derived. For a 2-D image, the surface points for the individual traces would be along a horizontal line, whereas for a 3-D image the surface points would be on a horizontal plane.

The word *interpretation* is subjected to many different meanings. In the final analysis, interpretation involves exercises of judgment based on geological and geophysical criteria. In the past ten years, the seismic interpreter has decided not to be satisfied with just the images produced in the seismic-processing stage. With the advent of readily available computer workstations, the interpreter now has access to powerful software tools that come under the title of *interpretive processing*. The interpreter can make use of these tools to enhance the pictures as provided by the seismic-processing stage. As a result, the interpreter can produce individualized maps and cross sections that emphasize particular aspects related to the geologic features in question. In a general sense, interpretive processing falls under the heading of *image enhancement*. The difference between interpretive processing and seismic processing may be summed up in this way. Seismic processing relies greatly on the use of the wave equation and all the related methods of dealing with traveling waves. Interpretive processing, although it takes into account its debt to the wave equation, makes use of a plethora of non-wave-equation techniques. Interpretive processing relies heavily on the use of various deterministic and statistical image-processing methods with certain seismic features factored in. The purpose of interpretive-type software is to convert the image of the geology as provided by seismic processing into an enhanced image that brings out various critical aspects of value to the interpreter. The enhanced geologic images, which can be displayed on an interpretive visualization computer system, are used for the final evaluation of drilling sites for new oil wells and for reservoir characterization.

A seismic attribute is represented by a mathematical or statistical operation that is applied to an array of data. A new array, called the *attribute array*, is produced. The use of various types of attributes yields displays that emphasize different features as the case warrants. For example, one attribute may reveal subsurface anomalies more clearly. Another attribute may be used as direct hydrocarbon indicators. There are many types of seismic attributes available.

Attributes were first introduced in geophysics for seismic processing (20). In 1950 the emphasis in the seismic exploration for oil was on the detection of reflections that could not be visually seen because of high noise levels. Because of the different offsets of the various detectors from the source (say, 250 ft for the detector for one trace versus 750 ft for the detector for another trace), a reflection from a subsurface interface (horizon) will generally hit one detector before the other. As a result, at the onset of a reflected event from a horizon with a contrasting dip, the two traces would become dissimilar. This fact could be exploited. Two traces could be compared for points of dissimilarity, and such points could indicate the presence of a reflected event that otherwise might be lost in noise. A dissimilarity attribute was required and the following one was chosen. An operator is designed to predict one trace from the other. At places where the two traces are similar to each other, the prediction error is small. At places where the two traces are dissimilar, the prediction error is large. The dissimilarity attribute is computed as the mean-square prediction error, so the attribute is a positive quantity.

This attribute gives a measure of the dissimilarity of two traces with respect to each other. The attribute has peaks at the places of high discontinuity. Peaks on the attribute curve indicate the presence of the reflections.

Today attribute analysis forms the backbone of interpretative processing. The input to an interpretive software system is the image provided by seismic processing. It is assumed that the processing has been done correctly so that the image represents the subsurface rock structure and stratigraphy, and no longer represents a seismic wavefield, as do the raw seismic records. The intricacies of seismic wave motion, and its conversion into an image by seismic processing, are now relegated to the background. Instead the interpreter seeks the best possible choice of a set of attributes that will enhance various features of the geology of interest.

Seismic stratigraphy involves the study of seismic data to describe the geologic depositional environments through an orderly approach to the interpretation of seismic reflections. Fundamental to this approach is an understanding of the effects of lithology and bed spacing on reflection parameters. The use of attributes such as amplitude, frequency, and continuity is a valuable tool in the interpretation of environments. The attribute of reflection amplitude contains information concerning velocity and density contrasts at individual interfaces as well as information on the extent of interbedding. The attribute of frequency is related to such geologic factors as the spacing of reflectors or lateral changes in interval velocity. An attribute that represents continuity of reflections would be closely associated with continuity of bedding. For example, continuous reflections would indicate widespread, layered deposits.

Seismic reflections come from subsurface interfaces (the horizons). The geologic images provided by seismic processing (e.g., the migrated records) will show these interfaces in their correct spatial positions. Seismic reflections do not generally come from faults, so the images will not generally show faults as such. As a result, in seismic interpretation the positions of faults are generally inferred from the breaks (or discontinuities) in the horizons on a seismic image. A major advance in interpretive processing was made in the introduction of the so-called coherence-cube method (21). Here the term *cube* refers to any 3-D array of data. The coherence-cube method occupies, as it were, a separate chapter in the history of interpretive processing. The method involves processing a given geologic image for the purpose of accentuating geologic discontinuities instead of the usual seismic reflections. Discontinuities include faults and some stratigraphic features. An algorithm is used to compare the similarity of nearby regions of the given 3-D image. Trace segments which are similar to its neighbors are assigned a low discontinuity value, while trace segments which are not similar to its neighbors are assigned a high discontinuity value. The final result is a discontinuity cube with fault surfaces enhanced and noise and coherent stratigraphic features attenuated.

As the input to the coherence-cube method, a 3-D volume (cube) of data is selected. Generally this selection would be a geologic image resulting from the seismic-processing stage, such as the migrated record. The discontinuity processing systematically cuts through the data volume, trace by trace, without regard to the geologic horizons. An attribute is computed that gives a measure of the data dissimilarity from trace to trace. The output is a new 3-D volume of data (the

enhanced image made up of dissimilarity attributes). This dissimilarity image reveals faults and other subtle stratigraphic changes that stand out as prominent anomalies in otherwise homogeneous data. Discontinuity processing gives a new way to view seismic data by revealing the degree of dissimilarity from trace to trace. Interpretation can be based on the image of dissimilarity as well as on the original geologic image. The use of both types of image makes interpretation easier and more reliable.

## CONCLUSION

In the past fifty years the seismic reflection method has evolved from the handiwork of a few dedicated geophysicists using relatively simple instruments to a highly sophisticated endeavor using the latest instrumentation and computer technology. The greatest innovations in the seismic method during these years have been in the area of digital seismic processing. The seismic method provides a reliable means to image the subsurface in three dimensions in order to locate petroleum reservoirs. Today seismic surveys give clear and accurate geologic pictures in great detail. As a result, many unnecessary development holes have been eliminated. Recoverable reserves worldwide have increased not only through the discovery of new oil fields but also through the detection of isolated reservoir pools that might otherwise be missed. The success of the seismic method in finding oil and natural gas attests to the value of digital signal processing.

## BIBLIOGRAPHY

1. N. Wiener, *Cybernetics*, New York: Wiley, 1948.
2. N. Wiener, *Extrapolation, Interpolation, and Smoothing of Stationary Time Series*, New York: Wiley, 1949.
3. E. A. Robinson, Predictive decomposition of time series with applications to seismic exploration, Ph.D. Thesis, M.I.T., 1954; *Geophysics*, **32**: 418–484, 1967.
4. E. A. Robinson, *Random Wavelets and Cybernetic Systems*, London: Charles Griffin, and New York: Macmillan, 1962.
5. H. W. Bode, *Network Analysis and Feedback Amplifier Design*, Princeton, NJ: Van Nostrand, 1945.
6. N. K. Bose, Linear time-invariant discrete-time systems, in S. K. Mitra and J. F. Kaiser (eds.), *Handbook for Digital Signal Processing*, New York: Wiley, 1993.
7. A. Grossman and J. Morlet, Decomposition of Hardy functions into square integrable wavelets of constant shape, *SIAM J. Math. Anal.*, **15**: 723–736, 1984.
8. S. L. Marple, *Digital Spectral Analysis with Applications*, Englewood Cliffs, NJ: Prentice Hall, 1987.
9. F. Abeles, Nouvelles formules relatives a la lumière réfléchiée et transmise par un empilement de lames à faces parallèles, *C. R. Acad. Sci.*, **223**: 891–893, 1946.
10. E. A. Robinson, Spectral approach to geophysical inversion by Lorentz, Fourier, and Radon transforms, *Proc. IEEE*, **70**: 1039–1054, 1982.
11. E. A. Robinson and H. Wold, Minimum-delay structure of least-squares and eo ipso predicting systems, in M. Rosenblatt (ed.), *Time Series Analysis*, New York: Wiley, 1963, pp. 192–196.
12. J. M. Mendel, *Maximum-Likelihood Deconvolution, A Journey into Model-Based Signal Processing*, Berlin: Springer-Verlag, 1990.
13. N. S. Neidell, Perceptions in seismic imaging: Kirchhoff migration operators in space and offset time, an appreciation, *Geophys., Leading Edge*, **16**: 1005–1006, 1997.
14. A. J. Berkhout, *Seismic Migration*, Amsterdam: Elsevier, 1982.
15. D. Gabor, A new microscopic principle, *Nature*, **161**: 777–778, 1948.
16. E. A. Robinson, Holistic migration, *Geophys., Leading Edge*, **17**: 313–320, 1998.
17. E. A. Robinson, *Seismic Velocity Analysis and the Convolutional Model*, Englewood Cliffs, NJ: Prentice-Hall, and Dordrecht, The Netherlands: D. Reidel, 1983.
18. L. Lines, Application of tomography to borehole and reflection seismology, *Geophysics, Leading Edge*, **10**: 7, 11–17, 1991.
19. R. R. Stewart, *Exploration Seismic Tomography*, Tulsa, OK: Society of Exploration Geophysicists, 1991.
20. G. P. Wadsworth et al., Detection of reflections on seismic records by linear operators, *Geophysics*, **18**: 539–586, 1953.
21. M. Bahorich and S. Farmer, The coherence cube, *Geophys., Leading Edge*, **14**: 1053–1058, 1995.

ENDERS A. ROBINSON  
Columbia University

**SELECTION, SOFTWARE.** See SOFTWARE SELECTION.